Rotational predissociation of (rare gas atom)–(slow rotating diatomic molecule) complexes

F. A. Gianturco, A. Palma, P. Villarreal, G. DelgadoBarrio, and O. Roncero

Citation: J. Chem. Phys. **87**, 1054 (1987); doi: 10.1063/1.453338
View online: http://dx.doi.org/10.1063/1.453338
View Table of Contents: http://jcp.aip.org/resource/1/JCPSA6/v87/i2
Published by the American Institute of Physics.

Rotational predissociation of (rare gas atom)–(slow rotating diatomic molecule) complexes

F. A. Gianturco[a] and A. Palma
Department of Chemistry, University of Rome. Città Universitaria, 00185 Rome, Italy

P. Villarreal, G. Delgado-Barrio, and O. Roncero
Istituto de Estructura de la Materia, CSIC, Serrano 123, 28006 Madrid, Spain

(Received 25 September 1986; accepted 25 February 1987)

We present an adiabatic angular approximation, closely related to the infinite order sudden approximation, to treat rotational predissociation of triatomic van der Waals complexes formed by a rare gas atom and a diatomic molecule that is treated as a rigid rotor. The metastable states of the complex are obtained as discrete solutions of the Schrödinger equation while the corresponding continuum solutions allow us to estimate the rates for rotational predissociation, within the framework of the Golden Rule approximation, after the relevant discrete-continuum dynamical couplings are calculated. Applications to the He–CO, He–N_2, and He–O_2 systems are presented.

I. INTRODUCTION

A weakly bound complex, or van der Waals (vdW) molecule, usually consists of groups of atoms or molecules which are held together by intermolecular attractions.[1] These relatively weak interactions are of the order of a few tens and up to ~ 100 wave numbers and are responsible for such phenomena as deviation of real gas mixtures behavior from ideality and for condensation of molecules into liquids and solids. The most popular class of vdW molecules, one that has attracted a great deal of experimental and theoretical attention, is the triatomic complex X···BC, where X represents a rare gas atom and BC a closed shell diatomic "target." Of particular interest has been the study of the mechanism by which the internal energy of BC, rotational and/or vibrational, is being transferrred to the vdW bond with the X atom, a process resulting in the dissociation of the complex into X and BC.[2,3] The study of the rotational predissociation (RP) aspect of the above process will be the subject of the present paper.

We have recently examined in detail the outcome of the RP mechanism for the He–CO system[4] by means of an accurate treatment of the corresponding collisional process that solves the relevant coupled equations and employs the resultant S-matrix elements to analyze the predissociating channels.[5] We also used in that case four different approximate procedures for estimating energy levels in the continuum so that they can guide the scattering calculations in selecting the most realistic range of collision energies where one should look for predissociating behavior.

Due to the character of this system, an adiabatic angular approach led to energy levels close to the exact ones, while a diabatic rotational approximation, successfully used in rare gas–fast rigid rotor complexes,[6–8] only provided a qualitative picture of the energetics of the molecule. Since the agreement between diabatic energies and exact ones was not satisfactory, a diabatic rotational decoupling is therefore not expected to describe correctly the dynamics of RP in rare gas–slow rigid rotor complexes.

In this work we present an adiabatic angular picture of both the energetics of the triatomic molecule and the dynamics of its RP process. The model is closely related to the rotational infinite order sudden approximation (IOSA) used in scattering problems.[9–11] It takes advantage of the presence of fast vibrational and slow rotational motions within the complex to decouple rotations from the vibration of the van der Waals bond, thus providing energy levels that, in the He–CO case, are in good agreement with the exact levels. This is in itself of great interest since, in particular, the efficiency in the scattering calculations of resonances strongly depends on the accuracy of the estimated energies. Furthermore, one can also obtain continuum states and extend the model to calculate the discrete-continuum couplings arising through the angular operators in the Hamiltonian. They are, in turn, used to estimate widths for RP in the framework of the Golden Rule approximation. Due to the approximations involved in our treatment, the agreement between the calculated widths using the adiabatic and the exact approaches is only qualitatively good while the general features of the RP mechanism are well described with a great saving of computational effort. The application of the present model to He–N_2 and He–O_2 systems is also discussed and a similar behavior of the results is found in both the latter cases.

It is worth mentioning at this point that a similar study on the photodissociation of He–I_2 complexes was already carried out a while ago[12(a)] using model potentials for both the I_2 stretch, the vdW stretching, and the binding motions. However, the present analysis employs for the first time the IOS decoupling in a different form and focuses on the RP processes via very *realistic anisotropic* potentials. The present systems also exhibit rotational motion of the diatomic species which is faster than in the I_2 case, thereby extending the test of the IOS model.

[a] Address for correspondence: Dipartimento di Chimica, Città Universitaria, 00185 Rome, Italy.

 0021-9606/87/141054-08$02.10

Section II reports the theoretical models employed and describes the various approximations, while Sec. III presents the results of the computations and discusses their physical significance.

II. THEORETICAL TREATMENT

We consider a triatomic van der Waals molecule X–BC, where X is a rare gas atom and BC a rigid rotor (RR) molecule. After separation of the center of mass of the whole system, the Hamiltonian for nuclear motion may be written as

$$H = -\frac{h^2}{2\mu}\frac{\partial^2}{\partial R^2} + \frac{h^2\mathbf{l}^2}{2\mu R^2} + B_e\mathbf{j}^2 + V(R,\theta), \tag{1}$$

where μ is the atom–diatom reduced mass, R is the distance between X and the center of mass of BC, while θ is the angle between the vector **R** and that corresponding to the diatomic bond which we will call **r**. In Eq. (1), **l** and **j** are the angular momentum operators associated with R and r, respectively, and B_e is the rotational constant of the BC rotor. The potential $V(R,\theta)$ represents the full van der Waals interaction. In order to obtain the spectrum of discrete states of the triatomic molecule as well as the various continua corresponding to the atomic and diatomic fragments, we follow a description close to that employed to study vibrational predissociation of the HeI_2 system.[12(a),12(b)] Whenever the stretching frequency of the van der Waals bond is large compared with the rotational constant B_e and the constant associated with the centrifugal motion, let us say $B_e = h^2/2\mu R^2$ where R is some reasonable mean value of the R distance, we may write the discrete wave functions as the product of a radial and weakly angular dependent function ϕ times an angular function F:

$$\Psi^{\rm dis}_{nm}(\mathbf{R},\hat{r}) \approx \phi_n(R;\theta)F_{nm}(\hat{R},\hat{r}), \tag{2}$$

where $\hat{R}$ and $\hat{r}$ are unit vectors in the **R** and **r** directions, respectively, with $\hat{r} = \mathbf{r}/r_e$ and r_e being the equilibrium distance at which the diatomic bond is kept frozen. The discrete wave functions depend now on the quantum numbers n and m associated to the van der Waals stretching and the bending or oscillation in θ, respectively. The angular adiabatic approximation thus consists in neglecting the θ dependence, of the ϕ functions that hence become "transparent" to the action of the angular momentum operators, i.e., one can write

$$\mathbf{l}^2\Psi^{\rm dis}_{nm} = \phi_n\mathbf{l}^2F_{nm}, \tag{3a}$$

$$\mathbf{j}^2\Psi^{\rm dis}_{nm} = \phi_n\mathbf{j}^2F_{nm}. \tag{3b}$$

The latter functions, therefore, are found as solutions of the one-dimensional equations obtained for each θ value chosen at an arbitrary orientation:

$$\left[-\frac{h^2}{2\mu}\frac{\partial^2}{\partial R^2} + V(R,\theta)\right]\phi_n(R;\theta) = W_n(\theta)\phi_n(R;\theta). \tag{4}$$

Substituting now Eq. (2) into the usual Schrödinger equation

$$H\Psi^{\rm dis}_{nm} = E_{nm}\Psi^{\rm dis}_{nm} \tag{5}$$

and using Eqs. (3) and (4) we obtain, after multiplication by ϕ^* and integration over R,

$$\left[-\frac{h^2}{4\mu}\{A_n(\theta),\mathbf{l}^2\} + B_e\mathbf{j}^2 + W_n(\theta)\right]F_{nm}(\hat{R},\hat{r}) = E_{nm}F_{nm}(\hat{R},\hat{r}), \tag{6}$$

where $\{\ ,\ \}$ represents the usual anticommutator and $A_n(\theta)$ represents the mean value of $1/R^2$ in the ϕ_n state, i.e.,

$$A_n(\theta) = \langle \phi_n(R;\theta) \left|\frac{1}{R^2}\right| \phi_n(R,\theta)\rangle . \tag{7}$$

The last integral is introduced in order to improve on the use of a simple average $\bar{R}$ value. Since this quantity no longer commutes with the l^2 operator, we are forced here to include the necessary symmetrization.[13] Note that, from Eq. (6), the angular dependent eigenvalues of Eq. (4), $W_n(\theta)$, become now effective potentials for the bending motion of the complex. In order to solve Eq. (6), we expand the F functions via the "body-fixed" (BF) rotational basis set[14–16]:

$$F_{nm}(\hat{R},\hat{r}) = \sum_{j\Omega} C^{(nm)}_{j\Omega}\langle\hat{R},\hat{r}|JMj\Omega\rangle \tag{8}$$

with

$$\langle\hat{R},\hat{r}|JMj\Omega\rangle = \left(\frac{2J+1}{4\pi}\right)^{1/2} D^{J*}_{M\Omega}(\phi_R,\theta_R,0)Y^{\Omega}_j(\theta,\phi), \tag{9}$$

where J is the quantum number associated to the total angular momentum $\mathbf{J} = \mathbf{j} + \mathbf{l}$, M corresponds to the projection of **J** on the space-fixed z axis, j is the quantum number associated to **j**, and Ω corresponds to the projection of **J** (or equally, of **j**) on the body-fixed z axis, i.e., **R**. The D are elements of the Wigner rotation matrix[17] and depend on the polar angles (θ_R,ϕ_R) of **R** in the space-fixed system of reference, while Y are spherical harmonic functions depending on the polar angles (θ,ϕ) of **r** in the BF reference system. The representation of the angular momentum operators in the BF reference basis set is well known from the literature[18]:

$$\langle JMj\Omega|\,\mathbf{j}^2|JMj'\Omega'\rangle = \delta_{jj'}\delta_{\Omega\Omega'}\,j(j+1), \tag{10a}$$

$$\langle JMj\Omega|\,\mathbf{l}^2|JMj'\Omega'\rangle = \delta_{jj'}\{\delta_{\Omega\Omega'}\,[J(J+1)+j(j+1)-2\Omega^2] - \delta_{\Omega\pm1,\Omega'}\,[J(J+1)-\Omega(\Omega\pm1)]^{1/2} \times [j(j+1)-\Omega(\Omega+1)]^{1/2}\}. \tag{10b}$$

The corresponding representation of the functions of θ, A_n, and W_n in that basis may be obtained by an expansion in terms of Legendre polynomials $P_\lambda(\cos\theta)$,

$$f_n(\theta) = \sum_\lambda a^n_\lambda P_\lambda(\cos\theta), \quad f = A, W \tag{11}$$

and by further using the coupling expression[18]:

$$\langle JMj\Omega|P_\lambda(\cos\theta)|JMj'\Omega'\rangle = \delta_{\Omega\Omega'}\left(\frac{2j'+1}{2j+j}\right)^{1/2}\cdot C(j'\lambda j;000)\cdot C(j'\lambda j;\Omega 0\Omega), \tag{12}$$

where $C(j_1j_2j_3;m_1m_2m_3)$ are Clebsh–Gordon coefficients.[17] In this way, diagonalization of Eq. (6) provides us

with the desired triatomic energies E_{nm} together with the coefficients $C_{j\Omega}^{(nm)}$ of expansion (8).

With regards to the continuum states which describe the atom plus the diatomic fragment we can now use the usual infinite order sudden approximation and write the wave function as follows[9–11]:

$$\Psi_{j\Omega,\epsilon,\bar{l}}^{\text{cont}}(\mathbf{R},\hat{r}) \approx \phi_{\epsilon,\bar{l}}(R;\theta) < \hat{R},\hat{r}|JMj\Omega\rangle , \tag{13}$$

where ϕ is solution of the equation

$$\left[-\frac{h^2}{2\mu}\frac{\partial^2}{\partial R^2} + V(R,\theta) + \frac{\bar{l}(\bar{l}+1)}{2\mu R^2} \right] \phi_{\epsilon,\bar{l}}(R;\theta) = \epsilon\phi_{\epsilon,\bar{l}}(R,\theta) \tag{14}$$

corresponding to the relative kinetic energy of the fragments ϵ. The energy of the continuum states is thus given by

$$E(j) = \epsilon + B_e j(j+1) . \tag{15}$$

From here on, we shall neglect the contribution of the centrifugal term in Eq. (14) by choosing $\bar{l} = 0$. The corresponding analysis with $\bar{l} \neq 0$ only complicates the notation in the following analytical development without adding any further insight. Now, the half-width for RP of a metastable level (n,m) may be calculated in the framework of the "Golden Rule" approximation as

$$\Gamma_{nm} = \Pi \sum_{j\Omega} | V_{nm\to j\Omega}^{\text{dc}} |^2 \tag{16}$$

where V^{dc} are the discrete-continuum couplings

$$V_{nm\to j\Omega}^{\text{dc}} = \langle \Psi_{j\Omega,\epsilon}^{\text{cont}}(\mathbf{R},\hat{r}) | H | \Psi_{nm}^{\text{dis}}(\mathbf{R},\hat{r}) \rangle \tag{17}$$

that are calculated on the energy shell:

$$\epsilon = E_{nm} - B_e j(j+1) . \tag{18}$$

Introducing the Hamiltonian (1) into Eq. (17) and taking into account the orthogonality of the $\phi_n(R;\theta)$ and of the $\phi_{\epsilon,\bar{l}=0}(R,\theta)$ functions, we may write the couplings, Eq. (17), as the sum of two terms, each of them arising from either the $\mathbf{j}^2$ or the $\mathbf{l}^2$ operators, i.e.,

$$V_{nm\to j\Omega}^{\text{dc}} = B_e \langle \Psi_{j\Omega,\epsilon}^{\text{cont}} | \mathbf{j}^2 | \Psi_{\text{nm}}^{\text{dis}} \rangle + \frac{h^2}{2\mu} \left\langle \psi_{j\Omega,\epsilon}^{\text{cont}} \left| \frac{\mathbf{l}^2}{R^2} \right| \Psi_{nm}^{\text{dis}} \right\rangle = V_1(\mathbf{j}^2) + V_2(\mathbf{l}^2) . \tag{19}$$

Note that if we choose $\bar{l} \neq 0$ in Eq. (14), an additional term must be accounted for in the above expression, involving the overlapping of the radial functions, i.e., an integral of the following type:

$$\langle JMj\Omega | \langle \phi_{\epsilon,\bar{l}}(R;\theta) | \phi_n(R;\theta) \rangle W_n(\theta) | F_{nm}(\hat{R},\hat{r}) \rangle .$$

One now expands the radial part of the discrete wave function in terms of Legendre polynomials

$$\phi_n(R;\theta) = \sum_k \alpha_k^{(n)}(R) P_K(\cos\theta) \tag{20}$$

and uses the explicit expression, Eq. (9), of the BF angular functions to rewrite the full wave function as

$$\Psi_{nm}^{\text{dis}} = \sum_{kj'\Omega'} \alpha_k^{(n)}(R) P_k(\cos\theta) C_{j'\Omega'}^{(nm)} \times \left(\frac{2J+j}{4\pi} \right)^{1/2} D_{m\Omega'}^{J*}(\phi_R,\theta_R,0) Y_j^{\Omega'}(\theta,\phi) . \tag{21}$$

Using now the following well-known relations among angular functions[17]:

$$P_K(\cos\theta) = \left(\frac{4\pi}{2k+1} \right)^{1/2} Y_k^0(\theta,\phi) , \tag{22}$$

$$Y_{j_1}^{m_1}(\theta,\phi) Y_{j_2}^{m_2}(\theta,\phi) = \sum_{j_3} \left[\frac{(2j_1+1)(2j_2+j)}{4\pi(2j_3+1)} \right]^{1/2} \times C(j_1 j_2 j_3; m_1, m_2 m_1+m_2) \times C(j_1 j_2 j_3; 000) Y_{j_3}^{m_3}(\theta,\phi) , \tag{23}$$

we obtain an appropriate expression for the discrete wave function

$$\Psi_{nm}^{\text{dis}}(\mathbf{R},\hat{r}) = \sum_k \alpha_k^{(n)}(R) \sum_{j\Omega'} C_{j\Omega'}^{(nm)} \sum_P \left(\frac{2j'+1}{2p+1} \right)^{1/2} C(kj'p;0\Omega'\Omega') \times C(kj'p;000) \langle \hat{R},\hat{r}|JMp\Omega' \rangle . \tag{24}$$

Hence, using Eq. (10a) we have

$$V_1(\mathbf{j}^2) = B_e \sum_{kj'\Omega'} C_{j'\Omega'}^{(nm)} \langle JMj\Omega | \langle \phi_\epsilon(R;\theta) | \alpha_k^{(n)}(R) \rangle \times \sum_P \left(\frac{2j'+1}{2p+1} \right)^{1/2} C(kj'p;0\Omega'\Omega') \times C(kj'p;000)\, p(p+1) | JMj'\Omega' \rangle . \tag{25}$$

By expanding again the radial integrals

$$\langle \phi_\epsilon(R;\theta) | \alpha_k^{(n)}(R) \rangle = \sum_\lambda f_{k\lambda}^{(n)}(\epsilon) P_\lambda(\cos\theta) , \tag{26}$$

by using the triangular condition for the Clebsh–Gordan coefficients as well as their symmetry property[17]:

$$C(j_1 j_2 j_3; m_1, m_2, m_3) = (-1)^{j_1+j_2+j_3} \times C(j_2 j_1 j_3; m_2, m_1, m_3) ,$$

and by further taking into account Eq. (12), we reach for the contribution of the $\mathbf{j}^2$ term to the discrete-continuum coupling the following result:

$$V_1(\mathbf{j}^2) = B_e \sum_{j'} C_{j'\Omega}^{(nm)} \sum_{k\lambda} f_{k\lambda}^{(n)}(\epsilon) \times \sum_{p=p_{\min}}^{p_{\max}} \left(\frac{2j'+1}{2j+1} \right)^{1/2} p(p+1) \times C(j'kp;\Omega 0\Omega) C(j'kp;000) \times C(p\lambda j;\Omega 0\Omega) C(p\lambda j;000) , \tag{27}$$

where

$$P_{\min} = \max(|k-j'|;|j-\lambda|)$$

and

$$P_{\max} = \min(k+j';j+\lambda) . \tag{28}$$

In a similar way, by expanding the integrals $\langle \phi_\epsilon(R;\theta) | 1/R^2 | \alpha_k^{(n)}(R) \rangle$ as follows:

$$\left\langle \phi_\epsilon(R;\theta) \left| \frac{1}{R^2} \right| \alpha_k^{(n)}(R) \right\rangle = \sum_\lambda g_{k\lambda}^{(n)}(\epsilon) P_\lambda(\cos\theta) , \tag{29}$$

and using Eq. (10b), the contribution of the second term may be written as

$$V_2(\mathrm{I}^2) = \frac{h^2}{2\mu} \sum_j \sum_{\Omega'=\Omega-1}^{\Omega+1} C_{j\Omega'}^{(nm)} \sum_{k\lambda} g_{k\lambda}^{(n)}(\epsilon) \times \sum_{P=P_{\min}}^{P_{\max}} \left(\frac{2j'+1}{2j+1}\right)^{1/2} \langle JMp\Omega|\mathrm{I}^2|JMp\Omega'\rangle \times C(j'kp;\Omega'0\Omega')C(j'kp;000) \times C(p\lambda j;\Omega 0\Omega)C(p\lambda j;000) . \quad (30)$$

Finally, by using Eqs. (27) and (30) we can write the relevant discrete-continuum couplings in a compact form as follows:

$$V_{mn\to j\Omega}^{\mathrm{dc}} = \sum_j \left(\frac{2j'+1}{2j+1}\right)^{1/2} \sum_{\Omega'=\Omega-1}^{\Omega+1} \sum_{k\lambda} \sum_{p=p_{\min}}^{P_{\max}} C(j'kp;\Omega'0\Omega') \times C(j'kp;000)C(p\lambda j;\Omega 0\Omega)C(p\lambda j;000) \times \{p(p+1)F_{k\lambda}^{(n)}(\epsilon)\delta_{\Omega\Omega'} + G_{k\lambda}^{(n)}(\epsilon)\langle JMp\Omega|\mathrm{I}^2|JMp\Omega'\rangle\} , \quad (31)$$

where

$$F_{k\lambda}^{(n)}(\epsilon) = B_e f_{k\lambda}^{(n)}(\epsilon) ,$$

$$G_{k\lambda}^{(n)}(\epsilon) = \frac{h^2}{2\mu} g_{k\lambda}^{(n)}(\epsilon) .$$

From Eq. (31) it can be seen that the rotational predissociation of the complex is induced by the anisotropy of the potential. In fact, for an isotropic potential, only $k=\lambda=0$ remain in that expression and the discrete-continuum couplings then vanish. In the spirit of the Golden Rule approximation, we can also calculate the partial half-widths for RP processes which exit into the $(j\Omega)$ channel as being given by

$$\Gamma_{nm\to j\Omega} = \Pi|V_{nm\to j\Omega}^{\mathrm{dc}}|^2 . \quad (32)$$

III. RESULTS

The model described above has been applied to the systems He–CO, He–N_2, and He–O_2. We have used the potential energy surfaces for their rigid-rotor representation of Thomas *et al.*[19] (He–CO), Gianturco *et al.*[20] (He–N_2), and Faubel *et al.*[21] (He–O_2). These complexes present stretching frequencies in the range $\sim$[10,20] cm^{-1}, and the rotational constants for the different rotors are 1.931 (CO), 1.998 (N_2), and 1.445 cm^{-1} (O_2). For all the three systems we have estimated a constant associated to the centrifugal motion that is almost the same for all of them, i.e., $\sim$0.30 cm^{-1}. Therefore, we may expect that an adiabatic decoupling of target rotations and van der Waals bond vibrations may be adequate in describing RP processes.

The potentials were written via the usual expansion in terms of Legendre polynomials P_λ,

$$V(R,\theta) = \sum_\lambda V_\lambda(R)P_\lambda(\cos\theta) \quad (33)$$

up to seven λ values (with only the even values for He–N_2 and He–O_2). In order to get a grid of points fine enough for numerical accuracy, spline interpolations were carried out in all cases. Furthermore, as described elsewhere,[4] we have considered an extension of the C_6 and C_8 coefficients for each $V_\lambda(R)$ in order to increase the radial range of the full interactions.

The relevant angular range, $[0,\pi]$ for He–CO and $[0,\pi/2]$ for the other cases, was divided into equally spaced sectors to solve Eqs. (4) and (14) at fixed angles. The convergence in the calculation of discrete levels was rapidly achieved by including 10 to 15 angles. However, up to 60 angles were needed to calculate convergent discrete-continuum couplings. The radial discrete equations (4) were efficiently solved by a mixed Truhlar and Numerov–Cooley procedure,[28] while continuum energy normalized solutions of Eq. (14) were calculated by outward Numerov propagation of the wave function and by matching it to a sine behavior at large distances.[8] The expansions in terms of Legendre polynomials were done by a collocation procedure, whereby the necessary quadratures were calculated by using a $h/3$ Simpson's rule, with h being the step size of integration.

In Fig. 1 we plot the only existing eigenvalue W for the He–CO system as function of θ that corresponds to a stretching quantum number $n=0$. As a consequence of the high anisotropy of this system, the W function shows a marked oscillatory behavior as a function of orientation. The ground triatomic levels $n=m=0$ for $J=0$ and 1 are also plotted in this figure, showing that the equilibrium of the complex is the induced in the main by the polarity of the CO bond. For all the possible states corresponding to total angular momenta $J=0$ and 1, and even parity, the energies and associated half-widths for rotational predissociation of the He–CO complex are listed in Table I. They are also compared with the exact calculations of Ref. 4.

For each triatomic level, the main diatomic rotational state involved is found by means of the dominant coefficient of expansion (8) and the squared value of that coefficient is also included in the table. In this way, the channel that supports the resonance can be identified and qualitatively provides the necessary physical picture which allows us to carry out the exact calculations. Only four levels were found in this system and, therefore, for diatomic excitations higher than $j=3$ the complex does not exist. These energies are close to the exact ones with the exception of that corresponding to $j=2$, that is overestimated by $\sim$0.27 cm^{-1}. The widths are only in qualitative agreement with the exact ones and always come out to be larger than the latters. It is not an entirely

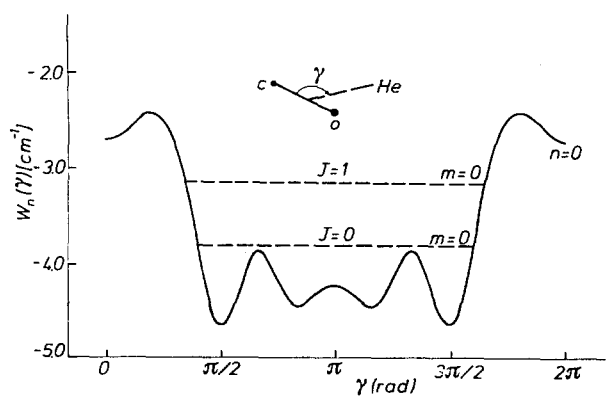

FIG. 1. Adiabatic angular potential (cm^{-1}) for the He–CO system. The two bound states (one for each) supported by the two lowest values of total angular momentum are shown.

TABLE I. He–CO system. Energies, partial and total half-widths for RP (in units of cm^{-1}) for $J(p) = 0(+)$. The dominant $|j\Omega\rangle$ diatomic state is also shown by indicating the highest coefficient in expansion (8). Rotational CO states included: $j = 0, 1, 2, 3, 4, 5$ in the exact calculations (Ref. 5).

$J(p) = 0(+)$	Adiabatic	Exact (Ref. 5)	$\left\|\frac{E^{AD} - E^{EX}}{E^{EX}}\right\| \cdot 100$	$\Gamma^{AD}/\Gamma^{EXACT}$
$(C^{nm=00}_{j\Omega=00})^2$	0.986			
$E_{j\Omega=00}$	−3.818			
$(C^{01}_{10})^2$	0.983			
E_{10}	0.922	0.939	2	
$\Gamma_{j\Omega=10\to j'\Omega'=00}$	0.461	0.281		1.6
$(C^{02}_{20})^2$	0.996			
E_{20}	9.301	9.037	3	
$\Gamma_{20\to00}$	0.434			
$\Gamma_{20\to30}$	0.582			
Γ_{20}	1.016	0.691		1.5
$(C^{03}_{30})^2$	0.999			
E_{30}	22.477	22.440	0.2	
$\Gamma_{30\to00}$	0.004			
$\Gamma_{30\to10}$	0.287			
$\Gamma_{30\to20}$	0.360			
Γ_{30}	0.651	0.585		1.1

surprising result if one considers the number of approximations involved in the present calculations, the most dubious being the use of the IOS approximation for very low energies and the neglect of discrete–discrete and continuum–continuum couplings. In fact, the agreement gets better whenever the kinetic energy between the fragments increases. It is however good to see that the model is able to predict the order of magnitude of the widths, that also describes correctly their relative distribution $\Gamma_{10} < \Gamma_{30} < \Gamma_{20}$ and that efficiently produces the rotational labels of the correct RP channels which need to be included. Further results for this system, corresponding to states with $J(p) = 1(+)$, are shown in Table II. With the exception of the only bound ground level, each level of $J(p) = 1(+)$ originates from the splitting of one level of $J(p) = 0(+)$, i.e., the one with the associated width of the same order of magnitude. For $j = 3$, only the level which corresponds to $\Omega = 1$ appears, since the splitting now carries the $\Omega = 0$ level to an energy higher than the diatomic threshold, and is therefore lost in the continuum. The energies and widths have in this case a similar behavior to that shown for the $J = 0$ case. However, for the $|j,\Omega\rangle = |1,1\rangle$ level, we see that the splitting locates it at an energy which is so low that its width becomes meaningless. On the other hand, the partial widths indicate a preference of the diatomic fragment to exit by the nearest open channel. Also, in the $J = 1$ case, a propensity to conserve the "tumbling" quantum number during the fragmentation may be observed. For He–N_2 and He–O_2, we plot in Fig. 2 the corresponding effective angular potentials W as functions of θ. In both cases, only the $n = 0$ stretching level appears at every angle. The potentials of this figure are much softer than that of Fig. 1, but the corresponding depths are also larger than in the former case, indicating once more that these systems have a similarly large anisotropy. We have also plotted in this figure the ground triatomic levels $n = m = 0$ corresponding to $J(p) = 0, 1(+)$ for both complexes. They show their equilibrium configurations to be around the T-shaped geometry and, in the He–N_2 case with $J = 0$, the bending motion is confined to take place within a narrow angular region. For He–O_2, the actual ground level corresponds to $J = 1$ because the only existing diatomic states are those with odd quantum numbers $j = 1,3,...$ as a consequence of the electronic configuration of O_2 in its ground state. For $J = 0$, the $n = m = 0$ level in He–O_2 is shifted from $\theta = \pi/2$, and O_2 rotates almost free within the complex.

For the He–N_2 case the presently computed energy levels and the corresponding half-widths for the RP mechanism are shown in Table III. The exact values obtained by solving the close-coupled (CC) equations of the scattering process are also reported. They correspond to even parity states, with $J = 0$ and 1 as do the approximate calculations of the table. The considered rotational states in the example calculated are those with odd quantum numbers, i.e., with $j = 1,3,5,...$. Obviously, the even-quantum rotational state also exist and give rise to an entirely similar pattern of rotational predissociation breakdown.

The general considerations which were made for the He–CO system are also applicable in the present case, although a few interesting differences are worth mentioning: Due to the increase of the rotational constant for the diatom the approximate energies are now less close to the exact ones, while the approximate Γ values are here reproducing very well the correct ones for a nonrotating complex but are less accurate as the total angular momentum increases. Moreover, the propensity for *not* conserving the Ω value is here exhibited by the computed widths, as opposed to what was shown by the He···CO example.

Finally, Table IV reports the present calculations for the He–O_2 system. In both cases odd rotational quantum

TABLE II. He–CO system. The same as in Table I but for the states with $J(p) = 1(+)$.

$J(p) = 1(+)$	Adiabatic	Exact	$\left\|\frac{E^{AD}-E^{EX}}{E^{EX}}\right\|\cdot 100$	$\Gamma^{AD}/\Gamma^{EXACT}$
$(C_{00}^{00})^2$	0.986			
E_{00}	−3.306			
$(C_{11}^{01})^2$	0.770			
E_{11}	0.094	0.301	68.8	
$\Gamma_{11\to 00}$	0.098	0.040		2.4
$(C_{10}^{02})^2$	0.763			
E_{10}	1.758	1.818	3	
$\Gamma_{10\to 00}$	0.307	0.205		1.5
$(C_{21}^{03})^2$	0.544			
E_{21}	8.485	8.512	0.3	
$\Gamma_{21\to 00}$	0.171			
$\Gamma_{21\to 10}$	0.011			
$\Gamma_{21\to 11}$	0.650			
Γ_{21}	0.832	0.580		1.4
$(C_{20}^{04})^2$	0.545			
E_{20}	10.860	10.756	1	
$\Gamma_{20\to 00}$	0.244			
$\Gamma_{20\to 10}$	0.171			
$\Gamma_{20\to 11}$	0.132			
Γ_{20}	0.547	0.428		1.3
$(C_{31}^{05})^2$	0.579			
E_{31}	20.987	21.059	0.3	
$\Gamma_{31\to 00}$	0.116			
$\Gamma_{31\to 10}$	0.040			
$\Gamma_{31\to 11}$	0.317			
$\Gamma_{31\to 20}$	0.092			
$\Gamma_{31\to 21}$	0.492			
Γ_{31}	1.057	0.962		1.1

numbers have been considered for the diatomic fragment as required by its symmetry. The present model now shows both energy positions and widths that are in very good agreement with the exact calculations, as the diatomic fragment is here the slowest of the RR examined and therefore the present adiabatic angular approximation provides a very adequate description of its RP mechanism.

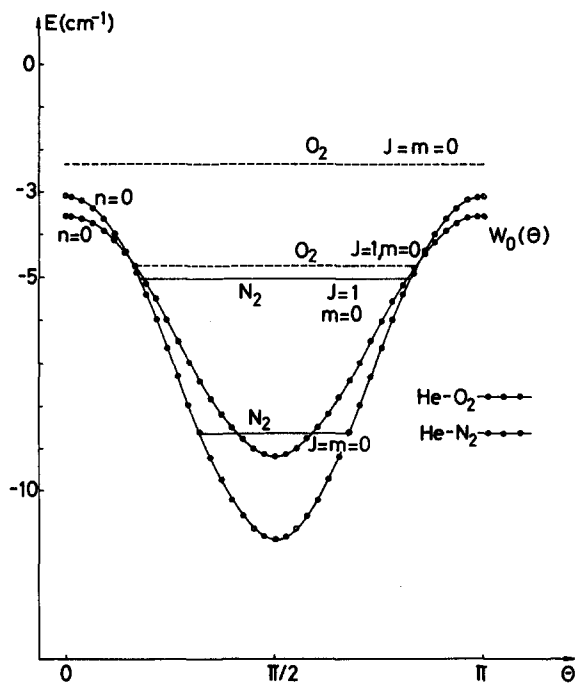

FIG. 2. Same as in Fig. 1 but for the He–O_2 and the He–N_2 systems. The corresponding bound state positions are also shown.

It is also instructive to examine the behavior of the rotationally diabatic[6] potential energy curves for the above systems as a function of the target rotational states. They provide a rather direct link, in fact, between the strength of the anisotropy in the interaction, as function of bond stretching along the vdW motion, and the coupling between target states that is given by such an interaction.

Figure 3 reports the shape of such inelastic (off-diagonal) potential curves for He–N_2 at $J_{tot} = 0$ and clearly shows the dominance of the $\Delta j = 2$ coupling over the other terms. In contrast, the He–CO system showed quite comparable couplings between the $j = 0$ state and the $j = 1$ and $j = 2$ state.[4]

The differences between the elastic coupling and the inelastic curves is shown in Fig. 4 for the He$\cdots$$O_2$ case, where one clearly sees that the rotationally diabatic approach does not realistically describe the present systems as it suggests very little off-diagonal coupling, hence much narrower RP widths than those shown by the present calculations. Figure 5, however, compares the relative strengths of the inelastic couplings for the same system and shows once more the dominance of the coupling between neighboring levels, as indicated by the He$\cdots$$N_2$ case. The coupling, on the other

TABLE III. He–N_2 system. Same as in the previous tables for $J(p) = 0.1(+)$. Rotational N_2 states included: $j = 1,3,...,11$.

$J(p) = 0(+)$	Adiabatic	Exact	$\left\lvert\frac{E^{AD} - E^{EX}}{E^{EX}}\right\rvert \cdot 100$	$\Gamma^{AD}/\Gamma^{EXACT}$
$(C_{10}^{00})^2$	0.993			
$(C_{30}^{01})^2$	− 1.728			
E_{30}	20.383	21.053	3	
$\Gamma_{30\to10}$	0.861	0.878		0.9
$J(p) = 1(+)$				
(C_{11}^{00})	0.954			
E_{11}	− 5.067			
$(C_{10}^{01})^2$	0.952			
E_{10}	− 1.047			
$(C_{31}^{02})^2$	0.604			
E_{31}	18.615	19.321	3.6	
$\Gamma_{31\to10}$	0.338			
$\Gamma_{31\to11}$	0.328			
Γ_{31}	0.666	0.857		0.8
$(C_{30}^{03})^2$	0.604			
E_{30}	22.376	22.923	2.4	
$\Gamma_{30\to10}$	0.036			
$\Gamma_{30\to11}$	0.210			
Γ_{30}	0.246	0.597		0.4

hand, appears here to be weaker than in the case of N_2 targets (see Fig. 3) and therefore qualitatively confirms the finding of smaller widths for the former system as compared with the latter shown by the present calculations of Tables III and IV.

In conclusion, we have presented an adiabatic angular model to treat the rotational predissociation of rare gas–diatomic molecules vdW complexes, whereby one takes advantage of the differences existing between the fast motion of the light rare gas along the vdW coordinate and the slower rotation of the diatom during the bending motion within the complex. The physical situations usually studied have belonged to a class of complexes at the other extreme of the scale, since they have involved fast rotors coupled to heavier rare gases,[23–25] and therefore the models developed for them[6,12] are wholly inadequate for the polyelectronic diato-

TABLE IV. He–O_2 system calculations similar to those of the previous tables. States considered: $J(p) = 0.1(+)$. Rotational diatomic states included in the calculation: $j = 1, 3, 5,...,11$.

$J(p) = 0(+)$	Adiabatic	Exact	$\left\lvert\frac{E^{AD} - E^{EX}}{E^{EX}}\right\rvert \cdot 100$	$\Gamma^{AD}/\Gamma^{EXACT}$
$(C_{10}^{00})^2$	0.994			
E_{10}	− 2.334			
$(C_{30}^{01})^2$	0.993			
E_{30}	14.543	14.780	1.6	
$\Gamma_{30\to10}$	0.623	0.581		1.1
$J(p) = 1(+)$				
$(C_{11}^{00})^2$	0.921			
E_{11}	− 4.759			
$(C_{10}^{01})^2$	0.920			
E_{10}	− 1.549			
$(C_{31}^{02})^2$	0.590			
E_{31}	12.740	13.049	2.4	
$\Gamma_{31\to10}$	0.247			
$\Gamma_{31\to11}$	0.288			
Γ_{31}	0.535	0.572		0.9
$(C_{30}^{03})^2$	0.591			
E_{30}	16.709	16.796	0.5	
$\Gamma_{30\to10}$	0.346			
$\Gamma_{30\to11}$	0.169			
Γ_{30}	0.515	0.403		1.3

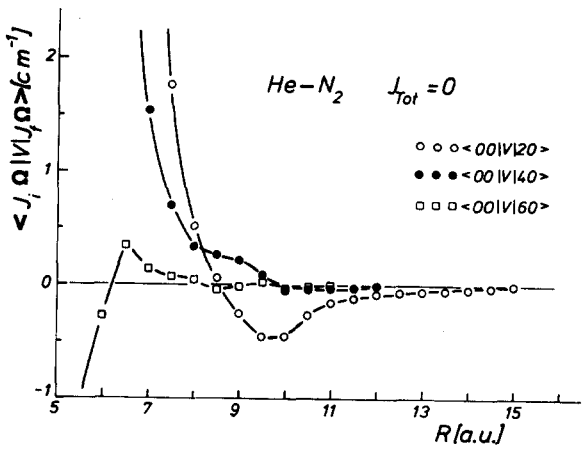

FIG. 3. Rotatonal diabatic potential curves for the off-diagonal, inelastic coupling in the case of the He–N_2 system with $J_{TOT} = 0$. The curves are labeled by the $|j\Omega\rangle$ states involved in the coupling.

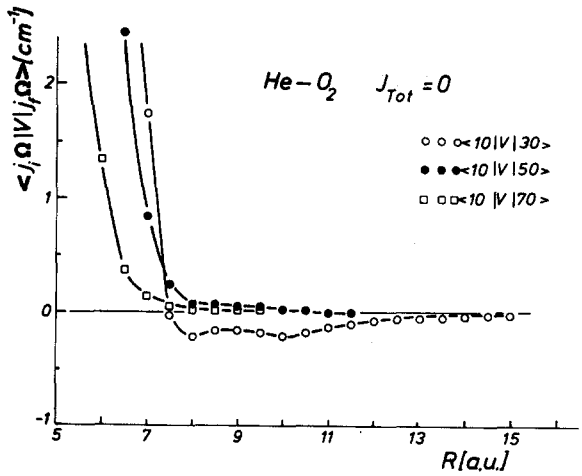

FIG. 5. Same as in Fig. 4, but on an enlarged energy scale to show the relative strengths of the off-diagonal coupling potentials for the He–O_2 case ($J_{TOT} = 0$).

mics studied here. On the other hand, the present inclusion of adiabaticity within the angular variables seems to catch the correct physics of the RP processes in these new complexes as the calculations show to predict energy levels very accurately and are therefore effective in guiding rigorous calculations that might be carried out in the region given by their estimates. The full coupling that controls half-width values, on the other hand, appears to be necessary to provide correct estimates for computed Γ's as the angular decoupling only provides qualitative agreement with exact, converged CC calculations. The fact that the correct order of magnitude was however given by the present model is already a further assurance of the basic validity of its physical assumptions, as it is well known that Γ calculations are very sensitive to the nature of the intracomplex coupling chosen to generate them.[24]

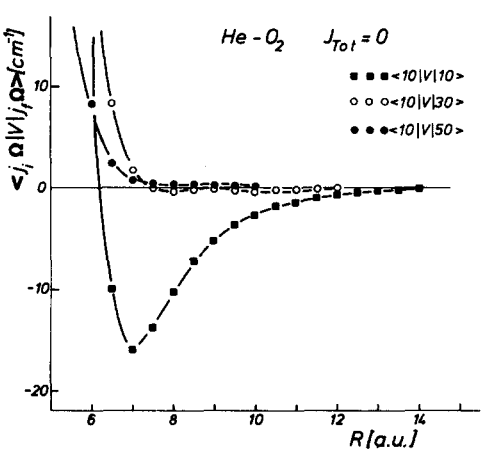

FIG. 4. Same as in Fig. 3 for the O_2–He system and including the main diagonal term within the diabatic model and with total angular momentum equal to zero.

ACKNOWLEDGMENTS

Two of us (G. D.-B. and P. V.) thank the University of Rome for a visiting fellowship during the tenure of which this work was begun. We also want to thank the referee for pointing out to us the work of Segev and Shapiro on the photodissociation of He–I_2 [Ref. 12(a)].

[1]For example, see D. M. Levy, Adv. Chem. Phys. **47**, 323 (1981).
[2]D. M. Levy, Science **214**, 263 (1981).
[3]S. B. Woodruff and D. L. Thompson, J. Chem. Phys. **71**, 376 (1979).
[4]F. A. Gianturco, A. Palma, G. Delgado-Barrio, P. Villarreal, and O. Roncero Phys. Rev. A (to be published).
[5]G. Delgado-Barrio, P. Villarreal, P. Mareca, and J. A. Beswick, Int. J. Quantum Chem. **27**, 173 (1985).
[6]J. A. Beswick and A. Requena, J. Chem. Phys. **72**, 3018 (1980).
[7]F. A. Gianturco, A. Palma, P. Villarreal, and G. Delgado-Barrio, Chem. Phys. Lett. **111**, 399 (1984).
[8]O. Roncero, S. Miret-Artés, G. Delgado-Barrio, and P. Villarreal, J. Chem. Phys. **85**, 2084 (1986).
[9]D. Secrest, J. Chem. Phys. **62**, 710 (1975).
[10]L. W. Hunter, J. Chem. Phys. **62**, 2855 (1975).
[11]L. Eno and G. G. Balint-Kurti, J. Chem. Phys. **71**, 1447 (1979).
[12](a) E. Segev and M. Shapiro, J. Chem. Phys. **78**, 4969 (1985); (b) J. A. Beswick and G. Delgado-Barrio, *ibid.* **73**, 3653 (1980).
[13]M. Aguado, P. Villarreal, G. Delgado-Barrio, P. Mareca, and J. A. Beswick, Chem. Phys. Lett. **102**, 227 (1983).
[14]C. F. Curtiss, J. O. Hirschfelder, and F. T. Adler, J. Chem. Phys. **18**, 1638 (1950).
[15]R. T Pack, J. Chem. Phys. **60**, 633 (1974).
[16]G. C. Schatz and A. Kuppermann, J. Chem. Phys. **65**, 4642 (1976).
[17]M. E. Rose, *Elementary Theory of Angular Momentum* (Wiley, New York, 1957).
[18]For example, see F. A. Gianturco, *The Transfer of Molecular Energy by Collisions* (Springer, Berlin, 1979).
[19]L. D. Thomas, W. P. Kraemer, and G. H. F. Diercksen, Chem. Phys. **51**, 131 (1980).
[20]F. A. Gianturco and A. Palma, J. Phys. B **18**, L519 (1985).
[21]M. Faubel, K. H. Kohl, J. P. Toennies, and F. A. Gianturco, J. Chem. Phys. **78**, 5629 (1983).
[22]See G. Delgado-Barrio, A. M. Cortina, A. Varadé, P. Mareca, P. Villarreal, and S. Miret-Artés, J. Comput. Chem. **7**, 208 (1986).
[23]C. J. Ashton, M. S. Child, and J. M. Hutson, J. Chem. Phys. **78**, 4025 (1983).
[24]J. M. Hutson and R. J. LeRoy, J. Chem. Phys. **78**, 4040 (1983).
[25]J. M. Hutson and B. J. Howard, Mol. Phys. **45**, 169 (1982).